

# Multiuser MISO PS-SWIPT Systems: Active or Passive RIS?

Shayan Zargari, Azar Hakimi, and Chintha Tellambura, *Fellow, IEEE*, Sanjeewa Herath, *Member, IEEE*

**Abstract**—Reconfigurable intelligent surface (RIS)-based communication networks promise to improve channel capacity and energy efficiency. However, the promised capacity gains could be negligible for passive RISs because of the double pathloss effect. Active RISs can overcome this issue because they have reflector elements with a low-cost amplifier. This letter studies the active RIS-aided simultaneous wireless information and power transfer (SWIPT) in a multiuser system. The users exploit power splitting (PS) to decode information and harvest energy simultaneously based on a realistic piecewise nonlinear energy harvesting model. The goal is to minimize the base station (BS) transmit power by optimizing its beamformers, PS ratios, and RIS phase shifts/amplification factors. The simulation results show significant improvements (e.g., 19% and 28%) with the maximum reflect power of 10 mW and 15 mW, respectively, compared to the passive RIS without higher computational complexity cost. We also show the robustness of the proposed algorithm against imperfect channel state information.

**Index Terms**—Reconfigurable intelligent surface (RIS), active RIS, simultaneous wireless information and power transfer, energy harvesting, beamforming.

## I. INTRODUCTION

A reconfigurable intelligent surface (RIS), a metasurface with numerous low-cost reflectors, can inherently manipulate the propagation environment to enhance energy and spectrum efficiency [1], [2]. RIS can be passive or active. The former imparts a phase change only, whereas the latter changes both the phase and amplitude of the incident radio frequency (RF) signal. Both types avoid expensive RF components, which are highly cost-effective. Thus, RIS may enable wireless fidelity (WiFi), navigation, and a plethora of applications [2]. Passive RIS and energy harvesting have also been considered [3]. However, the double pathloss from the product of the base station (BS)-RIS channel and the RIS-user channel limits the performance of the passive RIS networks [2]. Increasing the number of reflecting may mitigate this loss but drives up the cost. In response, active RIS has emerged [2], [4]–[6]. The active RIS includes a negative resistance so that the reflectors can not only reflect the RF signal but amplify it.

The benefits of active RISs have already been investigated [4], [5]. Reference [4] compares the active and passive RIS in a single-input multi-output (MISO) network and formulates the signal-to-noise ratios (SNRs). The spectral efficiency of the uplink is investigated in [7], where asymptotic and theoretical performance bounds are derived. [5] develops resource allocations for a multiuser network by minimizing the BS transmit power. Indoor and outdoor applications can deploy active

RIS-aided systems with energy harvesting (EH) requirements, such as smart homes and IoT networks. This deployment improves the network energy efficiency, a critical benefit. On the other, simultaneous wireless information and power transfer (SWIPT) can help the same goals [8]–[10].

This letter aims to quantify the benefits of active RIS by evaluating transmit power savings achieved by a network resulting from its use. Accordingly, we design the system with an active RIS (Fig. 1) to minimize the transmit power of the BS. This optimization problem involves the BS beamformers, power splitting (PS) ratios at the users, and active RIS phase shifts/amplification factors. This problem is non-convex because of variable entanglement. We thus leverage the block coordinate descent (BCD) method (also known as alternating optimization), which divides the variables into two alternating blocks. The first block comprises the BS beamformer weights and the PS ratios, and the second block comprises the active RIS phase shifts and amplification factors. The methods we use to solve them are convex relaxation and a penalty-based technique. We thus develop the intermediate power and phase shift algorithm (IPPA) and the overall BCD algorithm. We also show that performance gain for the active RIS over the passive RIS comes with no additional computational complexity cost.

*Notation:* Vectors and matrices are indicated by boldface lower-case and capital letters, respectively. For a square matrix  $\mathbf{A}$ ,  $\mathbf{A}^H$ ,  $\mathbf{A}^T$ ,  $\text{Tr}(\mathbf{A})$ ,  $\|\mathbf{A}\|_*$ , and  $\text{Rank}(\mathbf{A})$  denote its Hermitian conjugate transpose, transpose, trace, trace norm, and Rank, respectively.  $\mathbf{A} \succeq \mathbf{0}$  denotes a positive semidefinite matrix.  $\text{diag}(\cdot)$  is the diagonalization operation. The Euclidean norm of  $\mathbf{x}$  is  $\|\mathbf{x}\|$ , and the absolute value of  $x$  is  $|x|$ .  $\nabla_{\mathbf{x}}f(\mathbf{x})$  is the gradient vector over  $\mathbf{x}$ .  $\mathbb{E}[x]$  is the expectation of  $x$ . A circularly symmetric complex Gaussian (CSCG) random vector with mean  $\boldsymbol{\mu}$  and covariance matrix  $\mathbf{C}$  is denoted by  $\sim \mathcal{CM}(\boldsymbol{\mu}, \mathbf{C})$ .  $\mathbb{C}^{M \times N}$  indicates  $M \times N$  dimensional complex matrices.  $\mathcal{O}$  denotes the big-O notation.

## II. SYSTEM MODEL

We consider a downlink communication system with a  $M$  antennas BS and  $K$  single antenna users index by  $\mathcal{K} = \{1, \dots, K\}$ . We propose an active RIS with  $N$  reflecting elements to improve this communication link. At the users, the received signal is split for information decoding (ID) and EH. The BS uses each time-frequency resource block simultaneously for transmitting to all the users. The flat-fading channel gains from the BS-to-RIS, RIS-to-user  $k$ , and BS-to-user  $k$  are denoted by  $\mathbf{G} \in \mathbb{C}^{N \times M}$ ,  $\mathbf{h}_{r,k} \in \mathbb{C}^{N \times 1}$ , and  $\mathbf{h}_{b,k} \in \mathbb{C}^{M \times 1}$ , respectively. All the channels undergo quasi-static flat Rician fading and remain unchanged for several symbols [9]. We also assume the RIS controller acquires all the channel state information (CSI) during the channel estimation

S. Zargari, A. Hakimi, and C. Tellambura with the Department of Electrical and Computer Engineering, University of Alberta, Edmonton, AB, T6G 1H9, Canada (e-mail: zargari.hakimina.ct4@ualberta.ca).

S. Herath is with the Huawei Canada, 303 Terry Fox Drive, Suite 400, Ottawa, Ontario K2K 3J1 (e-mail: sanjeewa.herath@huawei.com).

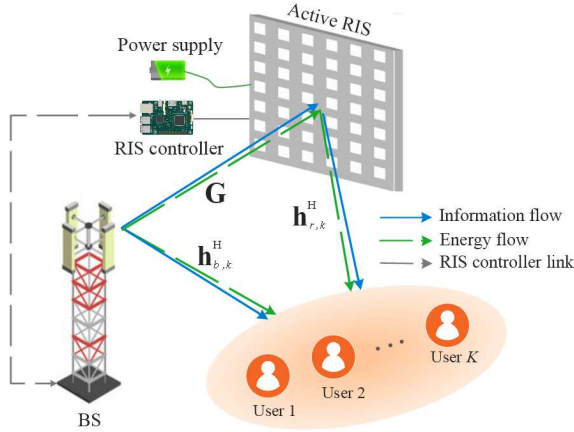


Figure 1: A multiuser MISO active RIS-assisted SWIPT system.

phase<sup>1</sup>. The system then adopts a codebook-based passive beamforming approach, where the RIS selects the best beam based on the received pilot sequences from the BS or users [1].

The signal model of  $N$  elements passive RIS is given by  $\mathbf{r} = \Theta \mathbf{x}$ , where  $\Theta = \text{diag}(e^{j\theta_1}, \dots, e^{j\theta_N})$  is the reflection-coefficients matrix at the RIS. With optimal RIS phase shifts, coherent combining at the user yields a high array gain proportional to  $N^2$ , a fundamental motivation of employing RIS [1]. However, when the direct link between the BS and the user is strong enough, the array gain becomes marginal [2]. This loss of efficacy happens because of the double pathloss effect, the product term of the BS-RIS channel and RIS-user channel. For a network at 5 GHz, 10,000 RIS elements are required to make the reflection link as strong as the direct link [2]. We thus consider an active RIS to overcome this issue. Unlike passive RIS, the active RIS can amplify the reflected signals<sup>2</sup>. Unlike full-duplex amplify-and-forward (FD-AF) relays, active RISs lack RF components and signal processing capabilities but only reflect and amplify the incident signals. Also, the performance of a FD-AF is limited by self-interference. Thus, a detailed comparison between these is an important future topic. Accordingly, the amplified and reflected signal of the active RIS [2], [5] can be represented as  $\mathbf{r} = \mathbf{P}\Theta \mathbf{x} + \mathbf{P}\Theta \mathbf{v} + \boldsymbol{\nu}$ , where  $\mathbf{P} = \text{diag}(p_1, \dots, p_N) \in \mathbb{R}^{N \times N}$  denotes the amplification factor matrix of the active RIS with each component greater than one. The second and third terms are dynamic and static noise at the active RIS. In addition,  $\mathbf{v} \sim \mathcal{CN}(\mathbf{0}_N, \sigma_v^2 \mathbf{I}_N)$  is related to the input noise and the inherent device noise of the active RIS elements, while the static noise  $\boldsymbol{\nu}$  is unrelated to  $\mathbf{P}$  and is negligible [2], [5].

### III. SYSTEM MODEL

The transmitted signal by the BS is given by  $\mathbf{x} = \sum_{i=1}^K \mathbf{w}_i s_i$ , where  $\mathbf{w}_i \in \mathbb{C}^{M \times 1}$ ,  $\forall i \in \mathcal{K}$ , denotes the BS

<sup>1</sup>If perfect CSI is not available, our results serve as theoretical performance upper bounds for the considered system. Robust versions of our algorithm can also be developed to reduce the effect of channel estimation errors, e.g., [10].

<sup>2</sup>To realize the active RIS platform, we assume an active reflection-type amplifier, which active elements can equip, e.g., current-inverting converters, asymmetric current mirrors, or some integrated circuits [2].

beamformers and  $s_i$  is the information symbol intended for user  $i$  which satisfies  $\mathbb{E}[|s_i|^2] = 1$ ,  $i \in \mathcal{K}$ . Then, the received signal at the active RIS is given by  $\tilde{\mathbf{r}} = \mathbf{P}\Theta \mathbf{G} \sum_{i=1}^K \mathbf{w}_i s_i + \mathbf{P}\Theta \mathbf{v}$ . Subsequently, the received signal at user  $k$  becomes  $y_k = \sum_{i=1}^K \mathbf{h}_k^H \mathbf{w}_i s_i + \mathbf{h}_{r,k}^H \mathbf{P}\Theta \mathbf{v} + z_k$ ,  $\forall k$ , where  $\mathbf{h}_k^H = \mathbf{h}_{r,k}^H \mathbf{P}\Theta \mathbf{G} + \mathbf{h}_{b,k}^H$  denotes the total channel gain from the BS to user  $k$ . Also,  $z_k \sim \mathcal{CN}(0, \sigma_k^2)$  is the received complex Gaussian noise at user  $k$ . By denoting  $\rho_k \in (0, 1)$  as the PS ratio, the received signal at each user is divided into two portions, where  $\rho_k$  portion is used for ID, and  $(1 - \rho_k)$  remaining portion is utilized for the EH. Consequently, the received signals for the ID and EH sections are given by  $y_k^{\text{ID}} = \sqrt{\rho_k} y_k + n_k$  and  $y_k^{\text{EH}} = \sqrt{1 - \rho_k} y_k$ , respectively, where  $n_k \sim \mathcal{CN}(0, \delta_k^2)$  is the additional noise introduced by the signal processing circuit of user  $k$  for the ID section [9]. Hence, the received signal-to-interference-plus-noise ratio (SINR) at user  $k$  can be written as

$$\text{SINR}_k = \frac{|\mathbf{h}_k^H \mathbf{w}_k|^2}{\sum_{\substack{i=1 \\ i \neq k}}^K |\mathbf{h}_k^H \mathbf{w}_i|^2 + \sigma_v^2 \|\mathbf{h}_{r,k}^H \mathbf{P}\Theta\|^2 + \sigma_k^2 + \frac{\delta_k^2}{\rho_k}}, \quad \forall k. \quad (1)$$

Practical EH circuits have two major drawbacks. First, the harvested energy does not linearly increase when the input power increases; instead, it saturates. Second, when the input power drops below the sensitivity level of the EH circuit, the harvested energy is zero [9], [10]. To capture these effects precisely, we employ the following piecewise nonlinear EH model [11]:  $P_{\text{EH}}^{\text{NL}} = \frac{aP_k^{\text{L}} + b}{P_k^{\text{L}} + c} - \frac{b}{c}$ , where  $P_k^{\text{L}}$  represents the linear input power to the EH section and  $a > 0$ ,  $b > 0$ , and  $c > 0$  capture the saturation and sensitivity thresholds of the EH circuit. By applying a best-fit match with experimental data,  $a$ ,  $b$ , and  $c$  can be estimated. The harvested energy at user  $k$  can then be written as  $P_k^{\text{L}} = \eta_k (1 - \rho_k) \left( \sum_{i=1}^K |\mathbf{h}_k^H \mathbf{w}_i|^2 + \sigma_v^2 \|\mathbf{h}_{r,k}^H \mathbf{P}\Theta\|^2 \right)$ ,  $\forall k$ , where  $\eta_k \in (0, 1]$  is the energy conversion efficiency. We assume  $\eta_k = 1$  for all users.

### IV. OPTIMIZATION PROBLEM

We aim to minimize the BS transmit power<sup>3</sup> by jointly optimizing the BS beamformers, PS ratios, and RIS phase shifts/amplification factors. The optimization problem can be formulated as

$$\text{(P1): } \underset{\mathbf{w}_k, \Theta, \mathbf{P}, \rho_k}{\text{minimize}} \quad f_1 = \sum_{k=1}^K \|\mathbf{w}_k\|_2^2, \quad (2a)$$

$$\text{s.t.} \quad \frac{|\mathbf{h}_k^H \mathbf{w}_k|^2}{\sum_{\substack{i=1 \\ i \neq k}}^K |\mathbf{h}_k^H \mathbf{w}_i|^2 + \sigma_v^2 \|\mathbf{h}_{r,k}^H \mathbf{P}\Theta\|^2 + \sigma_k^2 + \frac{\delta_k^2}{\rho_k}} \geq \gamma_k, \quad (2b)$$

<sup>3</sup>To realize the potential gain due to the use of an active RIS, a proper amount of power is allocated to each active RIS element from the total budget. Thus, compared to the passive RIS, the precise design of the BS beamformers is more important such that the quality of service for each user can be fulfilled, and the system power consumption is not excessive [5].

$$\sum_{i=1}^K \|\mathbf{P}\Theta\mathbf{G}\mathbf{w}_i\|^2 + \sigma_v^2 \|\mathbf{P}\Theta\|^2 \leq p_{\max}, \quad (2c)$$

$$P_{\text{EH}}^{\text{NL}} \geq e_k, \quad \forall k, \quad (2d)$$

$$0 < \rho_k < 1, \quad \forall k, \quad (2e)$$

where  $\gamma_k$  and  $e_k$  in (2b) and (2d) are the minimum SINR and harvested energy requirements at user  $k$ , respectively. Constraint (2c) indicates the power constraints at the active RIS with maximum reflect power,  $p_{\max}$ . Constraint (2e) denotes the PS ratio requirements. Following the similar approach in [9], we rewrite the right-hand side of constraint (2d) in a tractable form as follows:  $P_k^{\text{L}}(P_{\text{EH}}^{\text{NL}}) = \frac{b - (P_{\text{EH}}^{\text{NL}} + \frac{b}{c})c}{P_{\text{EH}}^{\text{NL}} + \frac{b}{c} - a}$ . Accordingly, (P1) can be recast as below

$$(P2): \underset{\mathbf{w}_k, \Theta, \mathbf{P}, \rho_k}{\text{minimize}} \quad f_1 = \sum_{k=1}^K \|\mathbf{w}_k\|_2^2, \quad (3a)$$

$$\text{s.t.} \quad (2b), (2c), (2e), \quad (3b)$$

$$\sum_{i=1}^K |\mathbf{h}_k^H \mathbf{w}_i|^2 + \sigma_v^2 \|\mathbf{h}_{r,k}^H \mathbf{P}\Theta\|^2 \geq \frac{P_k^{\text{L}}(e_k)}{1 - \rho_k}, \quad (3c)$$

(P2) is non-convex as the constraints contain entangled terms. Thus, we cannot solve it by standard popular convex software, e.g., CVX [12]. Therefore, we use a divide-and-conquer method, namely the BCD algorithm. First, we optimize the BS beamformers and PS ratios by applying semidefinite relaxation (SDR) and successive convex approximation (SCA). Second, we design the RIS phase shifts and amplification factors given the output of the first part. This process iterates until convergence.

#### A. Optimizing $\mathbf{w}_k$ and $\rho_k$ With Given $\Theta$ and $\mathbf{P}$

Since  $\mathbf{P}$  and  $\Theta$  appears in product form, we equivalently optimize  $\Upsilon = \mathbf{P}\Theta = \text{diag}(p_1 e^{j\theta_1}, \dots, p_N e^{j\theta_N})$  as the RIS precoding matrix that facilitates the optimization problem. By defining  $\mathbf{W}_k = \mathbf{w}_k \mathbf{w}_k^H$  and  $\mathbf{H}_k = \mathbf{h}_k \mathbf{h}_k^H \quad \forall k$ , we have

$$(P3): \underset{\mathbf{W}_k, \rho_k}{\text{minimize}} \quad f_2 = \sum_{k=1}^K \text{Tr}(\mathbf{W}_k), \quad (4a)$$

$$\text{s.t.} \quad \frac{\text{Tr}(\mathbf{H}_k \mathbf{W}_k)}{\gamma_k} - \sum_{\substack{i=1 \\ i \neq k}}^K \text{Tr}(\mathbf{H}_k \mathbf{W}_i) \geq \sigma_v^2 \|\mathbf{h}_{r,k}^H \Upsilon\|^2 + \tilde{\sigma}_k, \quad (4b)$$

$$\sum_{i=1}^K \text{Tr}(\Upsilon \mathbf{G} \mathbf{W}_i \mathbf{G}^H \Upsilon^H) + \sigma_v^2 \|\Upsilon\|^2 \leq p_{\max}, \quad (4c)$$

$$\sum_{i=1}^K \text{Tr}(\mathbf{H}_k \mathbf{W}_i) + \sigma_v^2 \|\mathbf{h}_{r,k}^H \Upsilon\|^2 \geq \frac{P_k^{\text{L}}(e_k)}{1 - \rho_k}, \quad (4d)$$

$$0 \leq \rho_k \leq 1, \quad \mathbf{W}_k \succeq 0, \quad \forall k, \quad (4e)$$

where  $\tilde{\sigma}_k := \sigma_k^2 + \frac{\delta_k^2}{\rho_k}$ ,  $\forall k \in \mathcal{K}$ . The rank-one constraint, i.e.,  $\text{Rank}(\mathbf{W}_k) \leq 1$ ,  $\forall k$ , is omitted to make (P3) a convex problem. (P3) is a standard semidefinite program (SDP) that can be solved efficiently by using CVX [12]. For all  $\mathbf{W}_k$ 's, it can be shown that the optimal solution to (P3) satisfies rank-one constraints [8]. Thus, eigenvalue decomposition (EVD) yields a globally optimal solution. The computational complexity of (P3) is given by  $\mathcal{O}(\sqrt{KM}(K^3 M^2 + K^2 M^3))$  [8].

#### B. Optimizing $\mathbf{P}$ and $\Theta$ with Given $\mathbf{w}_k$ and $\rho_k$

To design the RIS precoding matrix, we transform the optimization problem into a feasibility check problem. Let us first define  $\boldsymbol{\theta} = (p_1 e^{j\theta_1}, \dots, p_N e^{j\theta_N})^H \in \mathbb{C}^{N \times 1}$ . Furthermore, to make the problem more tractable, we apply the change of variables  $\mathbf{h}_{b,k}^H \mathbf{w}_i = a_{k,i}$ ,  $\mathbf{h}_{r,k}^H \Upsilon \mathbf{G} \mathbf{w}_i = \boldsymbol{\theta}^H \mathbf{b}_{k,i}$ , where  $\mathbf{b}_{k,i} = \text{diag}(\mathbf{h}_{r,k}^H) \mathbf{G} \mathbf{w}_i$ ,  $\mathbf{Q}_k = \text{diag}(\mathbf{G} \mathbf{w}_k) (\text{diag}(\mathbf{G} \mathbf{w}_k))^H$ , and  $\mathbf{Z}_k = \text{diag}(\mathbf{h}_{r,k}^H) \text{diag}(\mathbf{h}_{r,k})$ ,  $\forall k \in \mathcal{K}$ . Then, (P1) can be rewritten as follows

$$(P4): \text{Find } \boldsymbol{\theta}, \quad (5a)$$

$$\text{s.t.} \quad \frac{|\boldsymbol{\theta}^H \mathbf{b}_{k,k} + a_{k,k}|^2}{\sum_{\substack{j=1 \\ j \neq k}}^K |\boldsymbol{\theta}^H \mathbf{b}_{k,j} + a_{k,j}|^2 + \sigma_v^2 \boldsymbol{\theta}^H \mathbf{Z}_k \boldsymbol{\theta} + \tilde{\sigma}_k} \geq \gamma_k, \quad (5b)$$

$$\sum_{i=1}^K \boldsymbol{\theta}^H \mathbf{Q}_k \boldsymbol{\theta} + \sigma_v^2 \boldsymbol{\theta}^H \boldsymbol{\theta} \leq p_{\max}, \quad (5c)$$

$$\sum_{j=1}^K |\boldsymbol{\theta}^H \mathbf{b}_{k,j} + a_{k,j}|^2 + \sigma_v^2 \boldsymbol{\theta}^H \mathbf{Z}_k \boldsymbol{\theta} \geq \frac{P_k^{\text{L}}(e_k)}{1 - \rho_k}. \quad (5d)$$

Since (P4) holds quadratic inequality and equality constraints, the whole problem is non-convex. Hereafter, we use the SDR technique to transform (P4) into a convex problem. We introduce  $\tilde{\boldsymbol{\theta}} := [\boldsymbol{\theta}^T \ 1]^T \in \mathbb{C}^{(N+1) \times 1}$  and  $\mathbf{S}_{k,j} = [\mathbf{b}_{k,j} \mathbf{b}_{k,j}^H, \mathbf{b}_{k,j} a_{k,j}^H; \mathbf{b}_{k,j}^H a_{k,j}, 0]$ ,  $\forall i \in \mathcal{K}$ , respectively. Further, we define  $\mathbf{T} := \tilde{\boldsymbol{\theta}} \tilde{\boldsymbol{\theta}}^H \in \mathbb{C}^{(N+1) \times (N+1)}$ , which requires to satisfy  $\mathbf{T} \succeq \mathbf{0}$  and  $\text{Rank}(\mathbf{T}) = 1$ . Dropping the non-convex rank-one constraint, (P4) is relaxed into

$$(P5): \text{Find } \mathbf{T}, \quad (6a)$$

$$\text{s.t.} \quad \frac{\text{Tr}(\mathbf{S}_{k,k} \mathbf{T}) + |a_{k,k}|^2}{\gamma_k} - \sum_{\substack{j=1 \\ j \neq k}}^K \text{Tr}(\mathbf{S}_{k,j} \mathbf{T}) - \sigma_v^2 \text{Tr}(\tilde{\mathbf{Z}}_k \mathbf{T}) \geq \tilde{\sigma}_k, \quad (6b)$$

$$\sum_{i=1}^K \text{Tr}(\tilde{\mathbf{Q}}_k \mathbf{T}) + \sigma_v^2 \text{Tr}(\mathbf{T}) \leq p_{\max}, \quad (6c)$$

$$\sum_{j=1}^K \text{Tr}(\mathbf{S}_{k,j} \mathbf{T}) + |a_{k,j}|^2 + \sigma_v^2 \text{Tr}(\tilde{\mathbf{Z}}_k \mathbf{T}) \geq \frac{P_k^{\text{L}}(e_k)}{1 - \rho_k}, \quad (6d)$$

$$\mathbf{T} \succeq 0, \quad (6e)$$

where  $\tilde{\mathbf{Q}}_k$  and  $\tilde{\mathbf{Z}}_k$  are matrices with extra zero rows and columns. (P5) is an SDP that can be solved using CVX [12]. To achieve a rank-one solution, we exploit the penalty-based method [9], [10]. An equivalent form for the rank-one constraint can be written as  $\|\mathbf{T}\|_* - \|\mathbf{T}\|_2 \leq 0$ . We know that the inequality  $\|\mathbf{T}\|_* = \sum_i \sigma_i \geq \|\mathbf{T}\|_2 = \max_i \{\sigma_i\}$  holds for any given  $\mathbf{T} \in \mathbb{H}^{m \times n}$ , where  $\sigma_i$  is the  $i$ -th singular value of  $\mathbf{T}$ . The equality holds if and only if  $\mathbf{T}$  has rank-one. We thus have the following optimization problem:

$$(P6): \min_{\mathbf{T}} \quad \frac{1}{2\mu} (\|\mathbf{T}\|_* - \|\mathbf{T}\|_2), \quad \text{s.t.} \quad (6b) - (6e), \quad (7a)$$

---

**Algorithm 1** Intermediate power and phase shift Algorithm (IPPA)
 

---

**Input:** Set the iteration number  $j = 0$ , the convergence tolerance  $\zeta$ , and initialize  $\mathbf{T}^{(0)}$ .

- 1: **repeat**
- 2: Calculate  $\tilde{\Psi}(\mathbf{T})$  according to (8).
- 3: Solve (P7) to obtain  $\{\mathbf{T}^{(j)}\}$ .
- 4:  $j \leftarrow j + 1$ ;
- 5: **until**  $\frac{|f_3^{(j)} - f_3^{(j-1)}|}{f_3^{(j-1)}} \geq \zeta$

**Output:** return solution  $\{\mathbf{T}^*\}$ .

---



---

**Algorithm 2** Overall BCD Algorithm
 

---

**Input:** Set the iteration number  $i = 0$ , the convergence tolerance  $\zeta$ , and initialize  $\mathbf{T} = \mathbf{T}^{(0)}$ .

- 1: **repeat**
- 2: Solve (P3) for given  $\mathbf{T}^{(i)}$  to obtain  $\{\mathbf{W}_k^{(i)}, \rho_k^{(i)}\}$ .
- 3: Solve (P7) for given  $\{\mathbf{W}_k^{(i)}, \rho_k^{(i)}\}$  and denote the solution as  $\mathbf{T}^{(i+1)}$  based on Algorithm 1.
- 4: Set  $i \leftarrow i + 1$ ;
- 5: **until**  $\frac{|f_1^{(i)} - f_1^{(i-1)}|}{f_1^{(i-1)}} \geq \zeta$

**Output:** return solution  $\{\mathbf{T}^*\}$ .

---

where  $\mu$  is the penalty factor [9]. Specifically, for a sufficiently small value of  $\mu$ , solving (P6) yields a rank-one solution. However, (P6) is not convex as its objective function is the difference of two convex functions. To handle this, we resort to the SCA technique by approximating  $\Psi(\mathbf{T}) = \|\mathbf{T}\|_2$  with its first-order Taylor series expansion, which is a global lower bound as  $\Psi(\mathbf{T})$  is convex. The first-order Taylor series leads to

$$\Psi(\mathbf{T}) \geq \Psi(\mathbf{T}^i) + \text{Tr}\left(\nabla_{\mathbf{T}}^H \Psi(\mathbf{T}^i)(\mathbf{T} - \mathbf{T}^i)\right) \triangleq \tilde{\Psi}(\mathbf{T}), \quad (8)$$

where  $\nabla_{\mathbf{T}} \|\mathbf{T}^i\|_2 = \nabla_{\mathbf{T}} \mathbf{u}_1^H \mathbf{T}^i \mathbf{u}_1 = \nabla_{\mathbf{T}} \text{Tr}(\mathbf{T}^i \mathbf{u}_1 \mathbf{u}_1^H) = \mathbf{u}_1 \mathbf{u}_1^H$ , and  $\mathbf{u}_1$  is the eigenvector corresponding to the largest eigenvalue of  $\mathbf{T}^i$ . While (P6) contains an objective function, it is still a feasibility problem as any  $\mathbf{T}$  that has rank-one and satisfies the constraints is an optimal solution. Thus, we enforce an optimal solution that optimizes SINR and harvested energy margins while satisfying the rank-one constraint. To achieve this goal, we propose two new slack variables,  $\tau_k$  and  $\Delta_k$  as the ‘‘SINR residual’’ and ‘‘EH residual,’’ respectively [8]. The new formulated optimization problem is given by

$$(P7): \underset{\mathbf{T}, \tau_k, \Delta_k}{\text{minimize}} \quad f_3 = \frac{1}{2\mu} (\|\mathbf{T}\|_* - \tilde{\Psi}(\mathbf{T})) - \sum_{k=1}^K (\alpha \tau_k + \beta \Delta_k), \quad (9a)$$

$$\text{s.t. Modified-(6b), Modified-(6d), (6e),} \quad (9b)$$

$$\tau_k, \Delta_k \geq 0, \quad \forall k, \quad (9c)$$

where Modified-(6b) and Modified-(6d) are obtained from (6b) and (6d) by substituting  $\gamma_k$  with  $\gamma_k + \tau_k$  and  $P_k^L(e_k)$  with  $P_k^L(e_k) + \Delta_k$ ,  $\forall k \in \mathcal{K}$ , respectively. Besides,  $\alpha$  and  $\beta$  are positive constants. The feasible set for both problems (P6) and (P7) is the same. However, (P7) is more efficiently

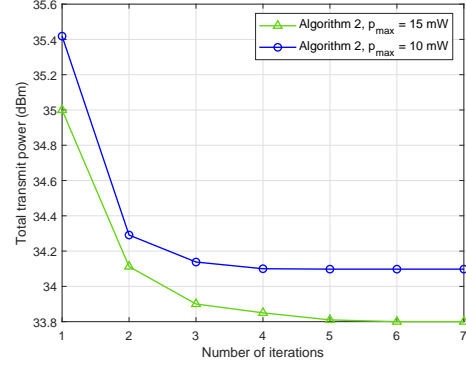


Figure 2: Convergence of Algorithm 2 ( $N = 20$  and  $M = 10$ ).

convergent [9]. The IPPA and the overall BCD algorithm are summarized in Algorithm 1 and Algorithm 2, respectively. The order of complexity for solving (P7) is given by  $\mathcal{O}(\log(1/\epsilon)((3K + 1)(N^{3.5} + 3KN^{2.5})))$ , where  $\epsilon > 0$  is the solution accuracy indicating that the active RIS does not have a higher computational complexity than the passive RIS [9]. Algorithm 2 iterations yield a non-increasing sequence of objective values for (P2) with guaranteed convergence. Let us consider  $\{\mathbf{w}_k, \rho_k\}$  and  $\boldsymbol{\theta}$  as the optimal solution of (P3) and (P7), respectively. Then, we have  $f_1(\boldsymbol{\theta}^{(i+1)}, \mathbf{w}_k^{(i+1)}, \rho_k^{(i+1)}) = f_1(\boldsymbol{\theta}^{(i)}, \mathbf{w}_k^{(i+1)}, \rho_k^{(i+1)}) \leq f_1(\boldsymbol{\theta}^{(i)}, \mathbf{w}_k^{(i)}, \rho_k^{(i)})$ . Equality arises as the objective is not a function of  $\boldsymbol{\theta}$ . So, as long as a feasible  $\boldsymbol{\theta}$  is selected, equality remains valid. Inequality comes from the fact that for given  $\boldsymbol{\theta}$ , the solutions  $\{\mathbf{w}_k, \rho_k\}$  are optimal. As for the convergence, we have a sequence of non-increasing objective values, which is guaranteed to converge.

## V. SIMULATION RESULTS

Here are the parameters of simulation results to evaluate Algorithm 2. The RIS has  $N$  active elements. All users are randomly located in a cluster with center (3.5, 8) meters (m) and radius 2.5 m. The AP location and the RIS location are considered as (3.5, 0) m and (0, 8) m, respectively. The Rician factor is set to 10 dB,  $K = 4$ ,  $\gamma_k = 10$  dB,  $p_{\max} = 10$  mW,  $e_k = -20$  dBm,  $\sigma_k^2 = -70$  dBm,  $\delta_k^2 = -50$  dBm,  $\sigma_v^2 = -70$  dBm,  $\zeta = 10^{-3}$ , and  $\mu = 5 \times 10^{-5}$  [9], [10]. The nonlinear EH model parameters are set to  $a = 2.463$ ,  $b = 1.635$ , and  $c = 0.826$  [11]. We consider the pathloss model  $L(d) = C_0(\frac{d}{D_0})^{-\kappa}$ , where  $C_0 = -30$  dB denotes the pathloss at the reference distance  $D_0 = 1$  m,  $d$  indicates the link distance and  $\kappa$  is the pathloss exponent, which is set to 3 and 2.2 for the direct and reflected links, respectively. For comparison, three benchmark system designs are studied, namely, 1) Algorithm 2 with different maximum reflect power; 2) Algorithm 2 with random PS ratio ( $\rho_{\text{rnd}}$ ); 3) Passive RIS; 4) Passive RIS with  $\rho_{\text{rnd}}$ ; 5) Passive RIS with random phase shifts ( $\theta_{\text{rnd}}$ ); 6) No RIS. For a fair comparison, the figures report the total transmit power as the sum of the BS and active RIS powers.

Fig. 2 shows the convergence behavior of Algorithm 2 for different maximum reflected power of the RIS,  $p_{\max}$ . All the curves converge to a stationary point within less than five iterations on average. Fig. (3a) plots the total transmit

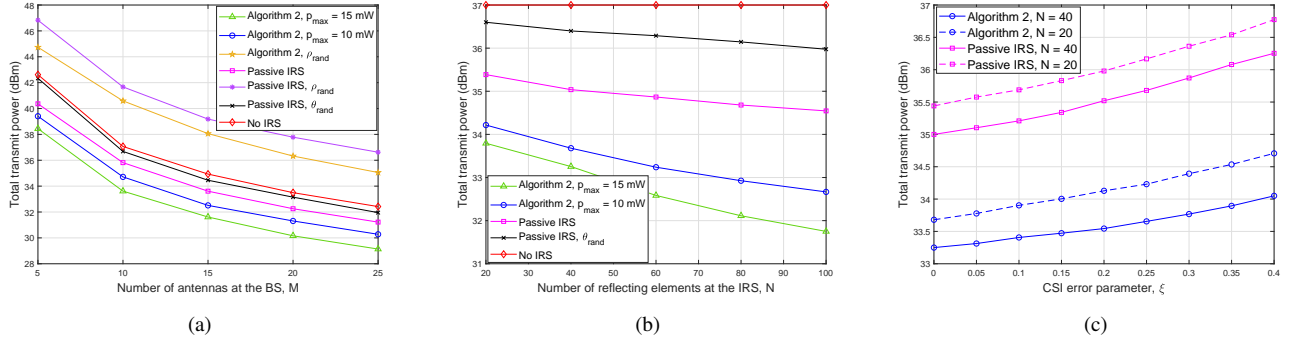


Figure 3: (3a) show the transmit power versus number of antenna at the BS,  $M$ , with  $N = 20$ . (3b) shows the transmit power versus number of active elements at the RIS,  $N$ , with  $M = 10$ . (3c) represents the transmit power versus CSI error parameter,  $\xi$ , with  $M = 10$  and  $p_{\max} = 15$  mW.

power versus the number of BS antennas,  $M$ , for different benchmarks. When  $M$  increases, the transmit power decreases for all the schemes. As well, Algorithm 2 outperforms others in terms of transmit power and achieves better performance by allocating more power to the active RIS. Thus, employing it further reduces the total transmit power given an additional maximum reflected power. However, it is significant to optimize  $\rho$  because  $\rho_{\text{rnd}}$  increases the transmit power.

Fig. (3b) represents the impact of the number of elements,  $N$ , at the active RIS on the total transmit power. As expected, sufficient reflectors at the active RIS cause transmit power reduction. When  $N$  grows, the multipath propagation between the BS and the users increases, leading to the enhancement of the received signal power at the user. Thus, to get the minimum required SINR for users, the power at the BS decreases. Indeed, with active RIS, the transmit power is reduced more due to the signal amplification at the RIS. This fact reveals that using the large or even massive elements at the active RIS can be advantageous for the MISO PS-SWIPT systems. Also, with  $N = 100$ , the active RIS with a maximum reflect power of 10 mW can save the transmit power 19% compared to the passive RIS. For the active RIS with a maximum reflect power of 15 mW, the gain is 28%.

Obtaining CSI is a critical challenge for wireless networks, and imperfect CSI is normal. Thus, it is important to study the robustness of Algorithm 2 to CSI error. For that, we use the following channel estimation model [10]:  $\hat{h} = h + e$ , where  $h$  is the real channel and  $e$  is the estimation error with Gaussian distribution and zero mean, i.e.,  $e \sim \mathcal{N}(0, \sigma_e^2)$ . We assume that the error variance satisfies  $\sigma_e^2 \triangleq \xi|h|^2$ , where  $\xi$  denotes the level of CSI error. Fig. (3c) shows the total transmit power versus  $\xi$ , indicating that the transmit power grows by increasing  $\xi$ . Specifically, for the active RIS scheme with  $N = 40$  and CSI error power of 10% of the channel gain (i.e.,  $\xi = 0.1$ ), the performance of Algorithm 2 experiences a loss of 5% compared to the ideal case without CSI error (i.e.,  $\xi = 0$ ). But, it exhibits strong robustness against CSI error.

## VI. CONCLUSIONS

This letter studied the transmit power minimization problem for a multiuser active RIS PS-SWIPT system. The BCD algorithm was developed to optimize the BS beamformers, RIS phase shifts/amplification factors, and PS ratios jointly.

Minimum requirements of data rate and harvested energy based on the piecewise nonlinear EH model were considered. We established the convergence of Algorithm 2 to a locally optimal solution. Simulation results demonstrated that the submitted designs perform better than the benchmarks. We found that active RIS helps to overcome the double pathloss effect and improve the EH capability of the users. It does so while decreasing the total transmit power. This letter serves as guidelines for many potential works on active RIS PS-SWIPT systems, e.g., prototype development, channel estimation, EH at the RIS, hardware design, and others.

## REFERENCES

- [1] M. D. Renzo, A. Zappone, M. Debbah, M. Alouini, C. Yuen, J. de Rosny, and S. A. Tretyakov, "Smart radio environments empowered by reconfigurable intelligent surfaces: How it works, state of research, and the road ahead," *IEEE J. Sel. Areas Commun.*, vol. 38, pp. 2450–2525, 2020.
- [2] Z. Zhang, L. Dai, X. Chen, C. Liu, F. Yang, R. Schober, and H. V. Poor, "Active RIS vs. passive RIS: which will prevail in 6G?," *CoRR*, vol. abs/2103.15154, 2021.
- [3] S. Hu, Z. Wei, Y. Cai, C. Liu, D. W. K. Ng, and J. Yuan, "Robust and secure sum-rate maximization for multiuser MISO downlink systems with self-sustainable irs," *IEEE Trans. Commun.*, vol. 69, no. 10, pp. 7032–7049, 2021.
- [4] R. Long, Y. Liang, Y. Pei, and E. G. Larsson, "Active reconfigurable intelligent surface-aided wireless communications," *IEEE Trans. Wirel. Commun.*, vol. 20, no. 8, pp. 4962–4975, 2021.
- [5] D. Xu, X. Yu, D. W. Kwan Ng, and R. Schober, "Resource allocation for active IRS-assisted multiuser communication systems," in *55th Asilomar Conference on Signals, Systems, and Computers*, pp. 113–119, 2021.
- [6] C. You and R. Zhang, "Wireless communication aided by intelligent reflecting surface: Active or passive?," *IEEE Wirel. Commun. Lett.*, vol. 10, no. 12, pp. 2659–2663, 2021.
- [7] M. Jung, W. Saad, and G. Kong, "Performance analysis of active large intelligent surfaces (LISs): Uplink spectral efficiency and pilot training," *IEEE Trans. Commun.*, vol. 69, no. 5, pp. 3379–3394, 2021.
- [8] S. Zargari, S. Farahmand, and B. Abolhassani, "Joint design of transmit beamforming, IRS platform, and power splitting SWIPT receivers for downlink cellular multiuser MISO," *Phys. Commun.*, vol. 48, 2021.
- [9] S. Zargari, A. Khalili, Q. Wu, M. R. Mili, and D. W. K. Ng, "Max-min fair energy-efficient beamforming design for intelligent reflecting surface-aided SWIPT systems with non-linear energy harvesting model," *IEEE Trans. Veh. Technol.*, vol. 70, no. 6, pp. 5848–5864, 2021.
- [10] S. Zargari, S. Farahmand, B. Abolhassani, and C. Tellambura, "Robust active and passive beamformer design for IRS-aided downlink MISO PS-SWIPT with a nonlinear energy harvesting model," *IEEE Trans. Green Commun. Netw.*, vol. 5, no. 4, pp. 2027–2041, 2021.
- [11] Y. Chen, N. Zhao, and M. Alouini, "Wireless energy harvesting using signals from multiple fading channels," *IEEE Trans. Commun.*, vol. 65, no. 11, pp. 5027–5039, 2017.
- [12] M. Grant, S. Boyd, and Y. Ye, "CVX: Matlab software for disciplined convex programming," 2009.